

Single pair of charge-2 Dirac and charge-2 Weyl phonons in GeO_2

Dong-Chang He(何东昌), Jia-Xi Liu(刘嘉希), Pei-Tao Liu(刘培涛), Jiang-Xu Li(李江旭), and Xing-Qiu Chen(陈星秋)
Citation: Chin. Phys. B, 2024, 33 (**10**): 100301. DOI: 10.1088/1674-1056/ad6a08
Journal homepage: http://cpb.iphy.ac.cn; http://iopscience.iop.org/cpb

What follows is a list of articles you may be interested in

Phase diagram and quench dynamics of a periodically driven Haldane model

Minxuan Ren(任民烜), Han Yang(杨焓), and Mingyuan Sun(孙明远)
Chin. Phys. B, 2024, 33 (**9**): 090309. DOI: 10.1088/1674-1056/ad4eb3

New approach to measuring topological phase transitions utilizing Floquet technology

Xue-Ying Yang(杨雪滢), Wei Wu(吴伟), and Ping-Xing Chen(陈平形)
Chin. Phys. B, 2024, 33 (**9**): 090305. DOI: 10.1088/1674-1056/ad5d94

Robust optical mode converter based on topological waveguide arrays

Yu-Xiang Xu(徐宇翔), Wen-Jian Tang(唐文剑), Li-Wei Jiang(姜力炜), De-Xing Wu(吴德兴), Heng Wang(王恒), Bing-Cong Xu(许冰聪), and Lin Chen(陈林)
Chin. Phys. B, 2024, 33 (**6**): 060306. DOI: 10.1088/1674-1056/ad3811

Topological laser on square lattice with gain-loss-induced higher-order corner modes

Ming-Jie Liao(廖明杰), Mei-Song Wei(韦梅松), Shuailing Wang(王帅领), Jingping Xu(许静平), and Yaping Yang(羊亚平)
Chin. Phys. B, 2024, 33 (**6**): 060305. DOI: 10.1088/1674-1056/ad322a

Peierls-phase-induced topological semimetals in an optical lattice: Moving of Dirac points, anisotropy of Dirac cones, and hidden symmetry protection

Jing-Min Hou(侯净敏)
Chin. Phys. B, 2020, 29 (**12**): 120305. DOI: 10.1088/1674-1056/abc0de

---

Single pair of charge-2 Dirac and charge-2 Weyl phonons in GeO_2

Dong-Chang He(何东昌)[1,2], Jia-Xi Liu(刘嘉希)[1,2], Pei-Tao Liu(刘培涛)[1], Jiang-Xu Li(李江旭)[1,†], and Xing-Qiu Chen(陈星秋)[1,‡]

[1] *Shenyang National Laboratory for Materials Science, Institute of Metal Research, Chinese Academy of Sciences, Shenyang* 110016, *China*
[2] *School of Materials Science and Engineering, University of Science and Technology of China, Shenyang* 110016, *China*

(Received 21 May 2024; revised manuscript received 19 July 2024; accepted manuscript online 1 August 2024)

The presence of a pair of Weyl and Dirac points (WP–DP) in topological semimetal states is intriguing and sought after due to the effects associated with chiral topological charges. However, identifying these states in real materials poses a significant challenge. In this study, by means of first-principles calculations we predict the coexistence of charge-2 Dirac and charge-2 Weyl phonons at high-symmetry points within a noncentrosymmetric $P4_12_12$ space group. Furthermore, we propose GeO_2 as an ideal candidate for realizing these states. Notably, we observe two distinct surface arcs that connect the Dirac and Weyl points across the entire Brillouin zone, which could facilitate their detection in future experimental investigations. This study not only presents a tangible material for experimentalists to explore the topological properties of WP–DP states but also opens up new avenues in the quest for ideal platforms to study chiral particles.

Keywords: topological phonon, Weyl points, Dirac points

PACS: 03.65.Vf **DOI:** 10.1088/1674-1056/ad6a08

1. Introduction

Topological quantum states, especially topological quasiparticles (e.g., Weyl and Dirac points), emerge around band degeneracy points in condensed matters and have attracted much attention in the past decade.[1–7] Nowadays, the concept of topology has been introduced into the field of phonon systems, giving impetus to the birth of topological phonons (TPs).[8–10] TPs characterized by topological invariants have emerged as an active research area in both theory and experiment in condensed matter physics and materials science. Phonons are the fundamental emergent bosons of crystalline lattices, describing the collective motion of the constituent atoms. Unlike fermions, they are not subject to the Pauli exclusion principle and Fermi surface constraints. The entire frequency range of the phonon dispersion can be experimentally observed and utilized to explore topological features. Similar to topological electrons, TPs have also been well studied and categorized into three types according to their degenerate dimensions. These include zero-dimensional (0D) nodal points (e.g., Weyl phonons,[11–22] Dirac phonons[23,24] and other high-degeneracy points[25,26]), one-dimensional (1D) nodal lines (e.g., nodal straight lines,[27–29] nodal rings,[30–33] nodal links,[34] nodal chains,[35,36] nodal cages,[37] nodal nets[38,39]), two-dimensional (2D) nodal surfaces (e.g., one-,[44–46] and two-[47] and three-nodal[48] surfaces). In particular, the coexistence[8,9,43,49,50] of different types of TP states in realistic materials has also attracted much attention.

Among these topological states, we focus on the nodal point states in this work. Weyl points (WPs) are a kind of more elementary fermions than Dirac points (DPs) to preserve the Lorentz symmetry, since a pair of WPs with opposite chiralities[51] can compose a DP. However, two identical WPs can be combined to form a Dirac point, which is referred to as "charge-2 Dirac point".[52,53] WPs behave like "magnetic" monopoles in momentum space whose charge is given by the chirality, and they are actually the source (monopole) and sink (antimonopole) of Berry curvature. In three-dimensional space, the component of Berry curvature in the z-direction is given by $\Omega_{xy}^{n} = \mathrm{i}\left(\left\langle\nabla_x n(R)|\nabla_y n(R)\right\rangle - \left\langle\nabla_y n(R)|\nabla_x n(R)\right\rangle\right)$. Berry curvature is an odd function in the presence of time-reversal symmetry ($\mathcal{T}$), and an even function in the presence of spatial inversion symmetry ($\mathcal{P}$). Consequently, in crystals where both time-reversal and spatial inversion symmetries are present, the Berry curvature vanishes across the entire Brillouin zone (BZ).[54] There are no topological charges, and no WPs, unless one of the two symmetries is broken, as depicted in Fig. 1(a). When the spatial inversion symmetry is broken, $\mathcal{T}$ does not change the topological charge. Assuming that a WP with charge $\mathcal{C}$ is located at point k in the BZ, then under $\mathcal{T}$ there is another WP at $-k$ with the same $\mathcal{C}$. According to the Nielsen–Ninomiya no-go theorem,[55] a net chiral charge cannot exist alone in the BZ, and thus there should be at least two pairs of WPs in the system to ensure the chiral charge neutrality. However, when the time-reversal symmetry is broken, $\mathcal{P}$ can change the sign of the topological charge and there can be only one pair of WPs. In the current research,[56–58] the system with only one pair of nodal states is usually found in magnetic materials. Whether this topological state can be found in a

†Corresponding author. E-mail: jxli15s@imr.ac.cn
‡Corresponding author. E-mail: xingqiu.chen@imr.ac.cn

© 2024 Chinese Physical Society and IOP Publishing Ltd

system with the existence of time-reversal symmetry is a topic of attention.

In this study, by employing symmetry analysis, we elucidate the mechanism of appearance of paired Weyl points and Dirac points, and their even topological charge. Additionally, we identify a real material GeO_2 in No. 92 space group which exhibits a minimum number of Weyl points and Dirac points in its phonon spectrum. Specifically, a pair of Weyl and Dirac points with a topological charge $\mathcal{C}$ of ± 2 appear at the high-symmetry points Γ and A, respectively. In addition, we confirm that the paired Weyl–Dirac points are situated over a wider frequency range compared to $BaPt_2S_3$[59] and their clear topological surface states span the entire BZ. Both features facilitate experimentalists to study their physical properties and surface state modes by spectroscopy experiments. Our work not only unveils exotic quasiparticles but also provides an ideal platform for investigating the entanglement between Dirac points and Weyl points.

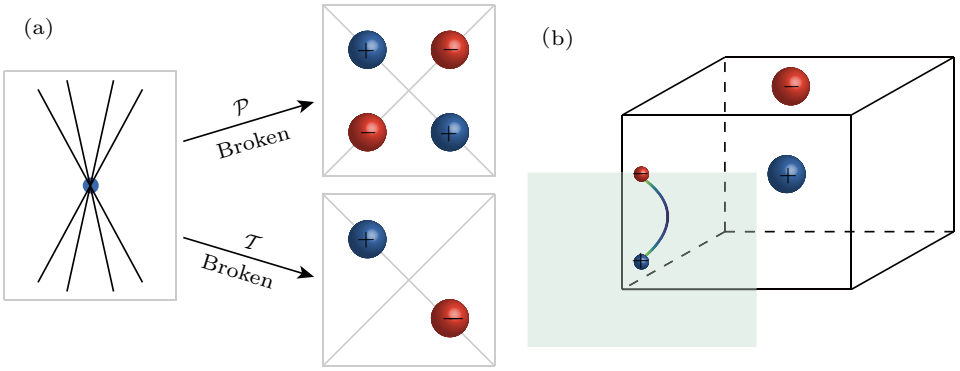


Fig. 1. (a) The relationship between Dirac points and Weyl points under $\mathcal{P}/\mathcal{T}$ symmetry breaking. (b) Projection of a WP at a high-symmetry point on a particular surface in the BZ, projection points are connected by Fermi arcs on specific surfaces.

2. Methods

First-principles calculations were performed using the Vienna *ab initio* simulation package (VASP)[61,62] based on the density functional theory (DFT).[63,64] The generalized gradient approximation parameterized by Perdew–Burke–Ernzerhof[65,66] was employed to describe the electron–electron interactions. The semi-core valence electrons were treated as valence electrons. The cutoff energy of the plane waves was set to 600 eV, and a Γ-centered $15\times15\times9$ k-point grid was used to sample the BZ. Atomic structure optimization was conducted until the remnant Hellmann–Feynman forces on the ions were less than 0.1 meV/Å. The force constants were computed with a $2\times2\times2$ supercell using the Phonopy package[67] based on the density functional perturbation theory.[68] The force constants were then taken as the tight-binding parameters to build the dynamic matrices. The surface phonon density of states (DOS) was obtained by using the surface iteration Green's function method[69] implemented in the home-developed TPHONON code.

3. Results and discussion

In phonon systems without spatial inversion symmetry, if WP was located at a general k point in BZ, then under $\mathcal{T}$ there are at least two pairs of WPs. However, if the first WP moved to a time-reversal-invariant momentum (TRIM) point, then k and $-k$ refer to the same point. When two WPs connected by time-reversal symmetry merge together, $\mathcal{T}$ would not lead to the WP doubling but an even topological charge occurs. This phenomenon has also been proven by contradiction in the work of Yang *et al.*[60] We also know that when considering WPs on TRIM points in spinful systems, $\mathcal{T}^2=-1$ dictates Kramer's degeneracy at all eight TRIM points in BZ, resulting in at least eight WPs. Spinless systems, on the other hand, do not have this constraint as $\mathcal{T}^2=1$. Therefore, even if the system has time-reversal symmetry, only one pair of WPs with opposite chiralities can exist. In addition, when WPs are projected onto a particular surface, a surface arc connecting the two projection points emerges, as illustrated in Fig. 1(b). Additionally, Dirac points in spinless systems also obey the above rules. Thus, we demonstrate that it is possible to realize a single pair of nodal points in spinless systems with time-reversal symmetry. To confirm our analysis, we carry out the real material GeO_2 as the example to study this intriguing phenomenon.

GeO_2 belongs to the noncentrosymmetric space group $P4_12_12$ (No. 92), which crystallizes in a simple tetragonal structure with 12 atoms in its primitive unit cell. The structure is depicted in Fig. 2(a), showing both a front and top view. In this structure, all Ge atoms occupy the 4*a* Wyckoff positions, while the O atoms occupy the 8*b* Wyckoff positions.

The optimized lattice parameters are $a=b=4.98$ Å and $c=7.19$ Å, which are close to the experimental values[70] of $a=b=4.99$ Å and $c=7.06$ Å. Figure 2(b) illustrates both the bulk BZ and the corresponding surface BZ. The yellow and green planes in the figure represent the projection of the (001) and (100) surfaces, respectively. The phonon band dispersions along the high-symmetry momentum paths are illustrated in

Fig. 2(c). The absence of imaginary phonon modes indicates the dynamic stability of the GeO_2 material. In Fig. 2(d), we plot the phonon band structure around 14 THz within a specific frequency range along the X–Γ–Z–A–R path as indicated by the highlighted area in Fig. 2(c). One can observe that the WP and DP at the TRIM point, respectively, formed by the crossing of two (Nos. 22 and 23) or four (Nos. 21–24) phonon branches, which are the only band degeneracies in the frequency range. Around the WP located at the high-symmetry point Γ, the band splitting exhibits linearity along the q_z direction and quadratic behavior in the q_x–q_y plane, consistent with its charge-2 character. Along the high-symmetry line Z–A, two doubly degenerate states converge, forming a fourfold degenerate point at the A point, exhibiting linear dispersion.

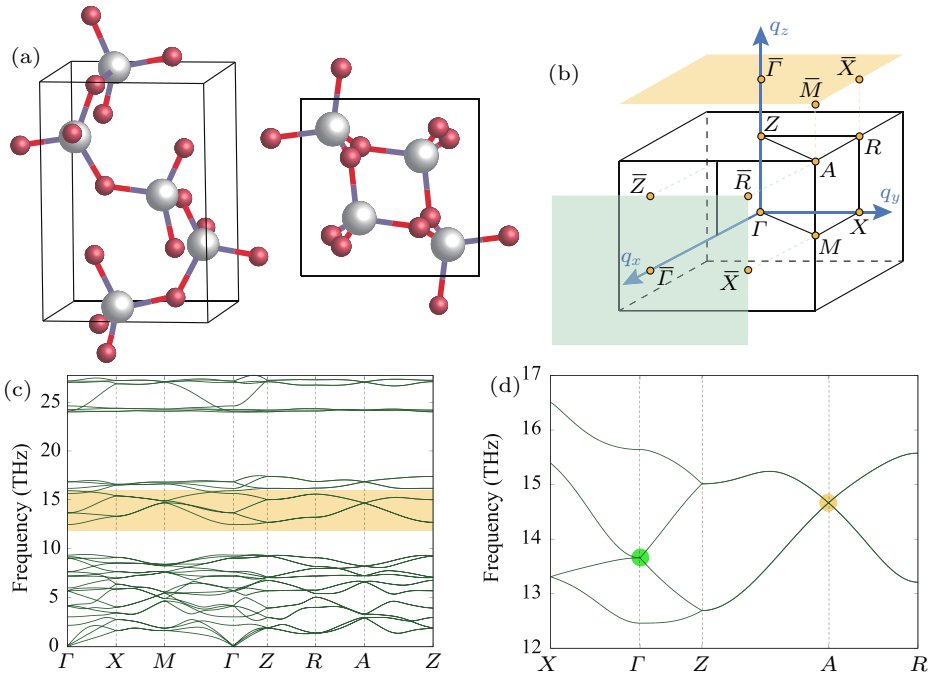


Fig. 2. (a) Side and top views of the crystal structure of GeO_2. The white and red spheres represent Ge and O atoms, respectively. (b) Bulk BZ and the (001) and (100) surface BZ of GeO_2. The corresponding high-symmetry points are marked. (c) The phonon dispersion of GeO_2 along the high-symmetry momentum paths in the BZ. (d) The enlarged image of band structure along the X–Γ–Z–A–R path in the yellow box highlighted in (c), in the 12.5–16 THz frequency region.

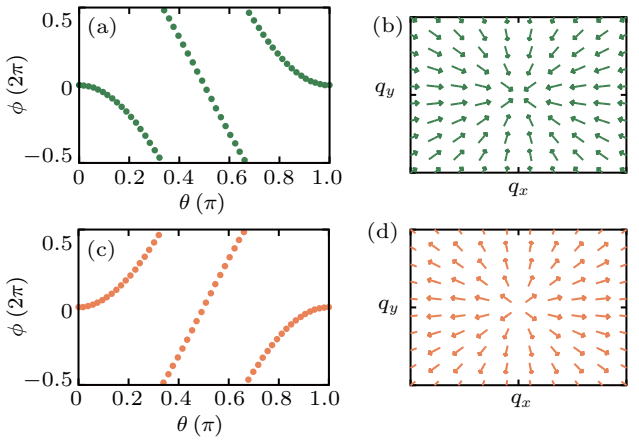


Fig. 3. (a) Wannier center evolution for two branches centered at the Γ point. (b) Berry curvature distributions of two branches centered at the Γ point. (c) Wannier center evolution for two branches centered at the A point. (d) Berry curvature distributions of two branches centered at the A point.

To determine the charge of the topologically protected nodes, we calculate the topological charge for the WP at Γ. Due to the well-separated bands, we can derive the Wannier center evolution for the WP. As depicted in Fig. 3(a), the Wannier center evolution for the corresponding branches indicate that they are topologically nontrivial. The WP at Γ possesses a high topological charge of -2. This is confirmed by the corresponding Berry curvature in the q_x–q_y plane, which exhibit sink behaviors at Γ as shown in Fig. 3(b). Similarly, we calculate the topological charge for the Dirac point located at A. Figure 3(c) demonstrates that the Wannier center evolution for the corresponding branches also indicate that they are topologically nontrivial, with a topological charge of $+2$, which is consistent with the prediction by Wang *et al.*[71] The corresponding Berry curvature in the q_x–q_y plane exhibits source behaviors at A, as depicted in Fig. 3(d). Based on these calculations, it is evident that the field is emitted from the Dirac point (positive charge) at A and absorbed by the WP (negative charge) at Γ.

Topological phonon nodal points with nonzero topological charge give rise to unique and nontrivial surface arcs. Consequently, we investigate the topological surface states associated with the WP–DP state in GeO_2 to explore their distinctive features. Initially, the DP possesses a nonzero topological charge with $\mathcal{C} = +2$. According to the principle of bulk–boundary correspondence,[72] this implies the existence of two surface states emerging from the surface projection of the DP.

Similarly, the topological charge of the WP at Γ is $\mathcal{C} = -2$, indicating the presence of two surface states connected to its surface projection. The total topological charge is 0, which satisfies the no-go theorem. Furthermore, since the projected WP resides at TRIM points, these two states must be time-reversal partners, meaning that one state is mapped to the other under the operation of $\mathcal{T}$ symmetry.

To explicitly demonstrate its nontrivial properties, using the iterative Green's function method we calculated the phonon local density of states (LDOS) and the corresponding isofrequency surface states projected on the (001) and (100) surfaces. Surface states in the phonon spectrum are clearly visible in the 13–15 THz frequency ranges. As shown in Fig. 4(a), two surface states can be observed emanating from the projected DP ($\overline{M}$), corresponding to the topological charge of DP. Figures 4(b) and 4(c) show isofrequency surface contours of the (001) surface at the frequencies of 13.8 THz and 14 THz, respectively, agree well with the phonon surface states observed in Fig. 4(a). These surface states reveal two surface arcs connecting the projected WP ($\overline{\Gamma}$) and DP ($\overline{M}$), with point A projecting onto $\overline{M}$. Moreover, the isofrequency surface states in Figs. 4(b) and 4(c) represent a noncontractible closed loop with a nontrivial winding around BZ. The phonon surface states span a large area in the surface BZ, making them accessible for experimental techniques such as angle-resolved photoemission spectroscopy or scanning tunneling spectroscopy. Similar behavior can be observed on the (100) surface, where point A projects onto $\overline{R}$, and two surface states can be observed emanating from the projected DP ($\overline{R}$). The corresponding isofrequency surfaces projected onto the (100) surface at 14 THz and 14.7 THz are shown in Figs. 4(e) and 4(f), respectively. The projection on both surfaces verifies the property that the topological charge is 2 for both Weyl and Dirac points.

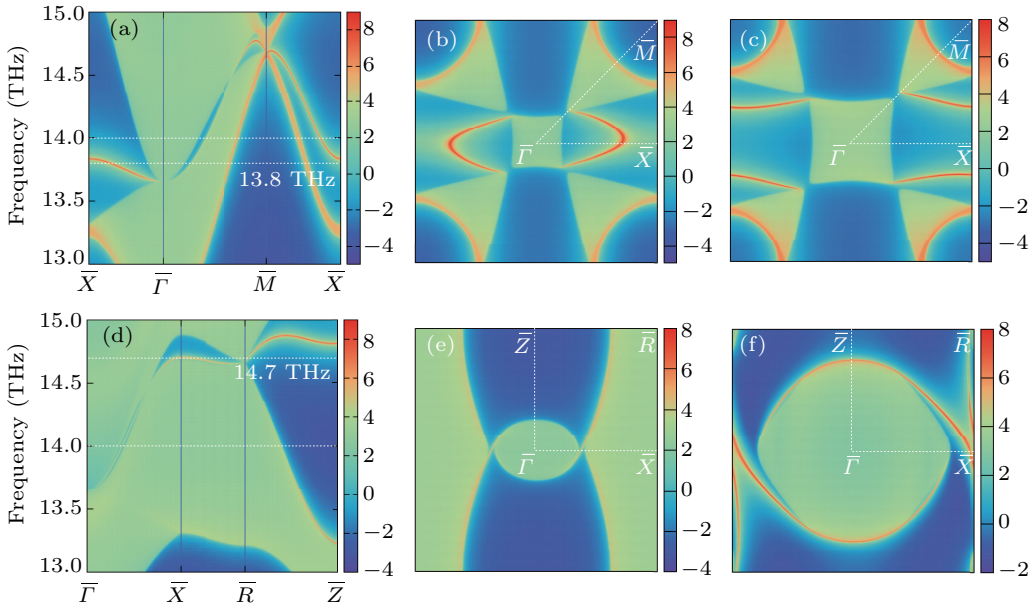


Fig. 4. Phonon surface states of GeO_2. (a) Phononic surface states along the high-symmetry lines for the (001) surface. (b) and (c) The isofrequency surfaces at $\omega = 13.8$ THz and 14 THz projected on the (001) surface, respectively. (d) Phononic surface states along the high-symmetry lines for the (100) surface. (e) and (f) The isofrequency surfaces at $\omega = 14$ THz and 14.7 THz projected on the (100) surface, respectively. In (b), (c) and (e), (f), the high-symmetry lines for LDOS are marked in white dashed lines.

4. Summary

In summary, we reveal the mechanism of single pair topological nodal points appearing in phonon spectrum and have investigated the topological surface states associated with a single pair of WP–DP states in a real spinless material system GeO_2 and demonstrated their unusual features. The DP carries a nonzero topological charge with $\mathcal{C} = +2$, leading to the existence of two surface states on the surface of the material. Similarly, the WP also has a chiral charge of two, resulting in two surface states connected to its surface projection. The clear surface arcs span the entire surface BZ, making them accessible for experimental detection. The bulk phonon of GeO_2 may be imaged by inelastic x-ray scattering[73] and neutron scattering.[74] The surface phonon modes may be verified by the high-resolution electron energy loss spectroscopy,[75,76] helium-atom scattering,[77] and THz spectroscopy.[44] Our work provides a real material for experimentalists in this field to study the topological properties of the WP–DP states. It also sheds light on the search for ideal platforms to study chiral particles.

Acknowledgements

Project supported by the National Key R&D Program of China (Grant No. 2021YFB3501503), the National Natural Science Foundation of China (Grant No. 51474202), Network and Information Foundation of CAS (Grant No. CAS-

WX2021SF-0102), and the Key Project of Chinese Academy of Sciences (Grant No. ZDRW-CN-2021-2-5). J. X. Li also acknowledges the funding from China Postdoctoral Science Foundation (Grant Nos. 2022T150660 and 2021M700152).

References

[1] Haldane F D M 2017 *Rev. Mod. Phys.* **89** 040502
[2] Chiu C K, Teo J C Y, Schnyder A P and Ryu S 2016 *Rev. Mod. Phys.* **88** 035005
[3] Goldman N, Budich J C and Zoller P 2016 *Nat. Phys.* **12** 7 639
[4] Armitage N P, Mele E J and Vishwanath A 2018 *Rev. Mod. Phys.* **90** 015001
[5] Wan X G, Turner A M, Vishwanath A and Savrasov S Y 2011 *Phys. Rev. B* **83** 205101
[6] Weng H M, Fang C, Fang Z, Bernevig B A and Dai X 2015 *Phys. Rev. X* **5** 011029
[7] Yu Z M, Zhang Z, Liu G B, Wu W, Li X P, Zhang R W, Yang S A and Yao Y G 2022 *Sci. Bull.* **67** 375
[8] Yu Z M, Zhang Z Y, Liu G B, Wu W K, Li X P, Zhang R W, Yang S Y A and Yao Y G 2022 *Sci. Bull.* **67** 4
[9] Li J X, Liu J X, Baronett S A, Liu M F, Wang L, Li R H, Chen Y, Li D Z, Zhu Q and Chen X Q 2021 *Nat. Commun.* **12** 1204
[10] Liu Y Z, Zou N L, Zhao S B, Chen X B, Xu Y and Duan W H 2022 *Nano Lett.* **22** 2120
[11] Li J X, Xie Q, Ullah S, Li R H, Ma H, Li D Z, Li Y Y and Chen X Q 2018 *Phys. Rev. B* **97** 054305
[12] Xie Q, Li J X, Ullah S, Li R H, Wang L, Li D Z, Li Y Y, Yunoki S and Chen X Q 2019 *Phys. Rev. B* **99** 174306
[13] Zhang T T, Song Z D, Alexandradinata A, Weng H M, Fang C, Lu L and Fang Z 2018 *Phys. Rev. Lett.* **120** 016401
[14] Miao H, Zhang T T, Wang L, Meyers D, Said A H, Wang Y L, Shi Y G, Weng H M, Fang Z and Dean M P M 2018 *Phys. Rev. Lett.* **121** 035302
[15] Ding G Q, Zhou F, Zhang Z Y, Yu Z M and Wang X T 2022 *Phys. Rev. B* **105** 134303
[16] Liu Q B, Wang Z J and Fu H H 2021 *Phys. Rev. B* **103** L161303
[17] Liu P F, Li J, Tu X H, Li H, Zhang J, Zhang P, Gao Q and Wang B T 2021 *Phys. Rev. B* **103** 094306
[18] Zhang T, Takahashi R, Fang C and Murakami S 2020 *Phys. Rev. B* **102** 125148
[19] Wang R, Xia B W, Chen Z J, Zheng B B, Zhao Y J and Xu H 2020 *Phys. Rev. Lett.* **124** 105303
[20] Huang Z Q, Chen Z J, Zheng B B and Xu H 2020 *npj Comput. Mater.* **6** 87
[21] Xia B W, Wang R, Chen Z J, Zhao Y J and Xu H 2019 *Phys. Rev. Lett.* **123** 065501
[22] Liu J, Hou W J, Wang E, Zhang S J, Sun J T and Meng S 2019 *Phys. Rev. B* **100** 081204
[23] Chen Z J, Wang R, Xia B W, Zheng B B, Jin Y J, Zhao Y J and Xu H 2021 *Phys. Rev. Lett.* **126** 185301
[24] Jin Y J, Wang R and Xu H 2018 *Nano Lett.* **18** 7755
[25] Yang T, Xie C, Chen H, Wang X and Zhang G 2022 *Phys. Rev. B* **105** 094310
[26] Zhong M, Liu Y, Zhou F, Kuang M, Yang T, Wang X and Zhang G 2021 *Phys. Rev. B* **104** 085118
[27] Li J, Xie Q, Liu J, Li R, Liu M, Wang L, Li D, Li Y and Chen X Q 2020 *Phys. Rev. B* **101** 024301
[28] Kang X Y, Li J Y, Li S 2023 *Chin. Phys. B* **32** 116301
[29] Liu G, Jin Y, Chen Z and Xu H 2021 *Phys. Rev. B* **104** 024304
[30] Jin Y J, Chen Z J, Xia B W, Zhao Y J, Wang R and Xu H 2018 *Phys. Rev. B* **98** 220103
[31] Zheng B, Xia B, Wang R, Chen Z, Zhao J, Zhao Y and Xu H 2020 *Phys. Rev. B* **101** 100303
[32] Zheng B, Zhan F, Wu X, Wang R and Fan J 2021 *Phys. Rev. B* **104** L060301
[33] Li J, Wang L, Liu J, Li R, Zhang Z and Chen X Q 2020 *Phys. Rev. B* **101** 081403
[34] Liu Q B, Fu H H and Wu R 2021 *Phys. Rev. B* **104** 045409
[35] Chen Y S, Huang F F, Zhou P, Ma Z S and Sun L Z 2021 *New J. Phys.* **23** 103043
[36] Zhu J, Wu W, Zhao J, Chen H, Zhang L and Yang S A 2022 *npj Quantum Mater.* **7** 2397
[37] Wang M, Wang Y, Yang Z, Fan J, Zheng B, Wang R and Wu X 2022 *Phys. Rev. B* **105** 174309
[38] Ding G, Sun T and Wang X 2022 *Phys. Chem. Chem. Phys.* **24** 11175
[39] Li W, Li Z, Pan B, Zhou P and Sun L 2023 *Physica Status Solidi RRL* **17** 2300048
[40] Yang T, Gu Q J, Wang P, Wu Z M and Zhang Z Y 2022 *Appl. Phys. Lett.* **121** 053102
[41] Zhang T T, Miao H, Wang Q, Lin J Q, Cao Y, Fabbris G, Said A H, Liu X, Lei H C, Fang Z, Weng H M and Dean M P M 2019 *Phys. Rev. Lett.* **123** 245302
[42] Liu Q B, Fu H H and Wu R Q 2022 *Phys. Chem. Chem. Phys.* **24** 17210
[43] Wang J H, Yuan H K, Yu Z M, Zhang Z Y and Wang X T 2022 *Phys. Rev. M* **5** 124203
[44] Wang X T, Zhou F, Yang T, Kuang M Q, Yu Z M and Zhang G 2021 *Phys. Rev. B* **104** L041104
[45] Wang J H, Yuan H K, Liu Y, Zhou F, Wang X T and Zhang G 2022 *Phys. Chem. Chem. Phys.* **24** 2752
[46] Liu Q B, Wang Z Q and Fu H H 2021 *Phys. Rev. B* **104** L041405
[47] Xie C W, Yuan H K, Liu Y and Wang X T 2022 *Phys. Rev. B* **105** 054307
[48] Xie C W, Yuan H K, Liu Y, Wang X T and Zhang G 2021 *Phys. Rev. B* **104** 134303
[49] Liu G, Huang Z Q, Chen Z J, Jin Y J, He C C and Xu H 2022 *Phys. Rev. B* **106** 054306
[50] Liu J, Liu P, Sun Y, Chen X Q and Li J 2023 *Phys. Rev. B* **108** 104312
[51] Weyl H 1929 *Z. Physik* **56** 330
[52] Geilhufe R M, Borysov S S and Bouhon A 2017 *Sci. Rep.* **7** 7298
[53] Zhang T T, Song Z D, Alexandradinata A, Weng H M, Fang C, Lu L and Fang Z 2018 *Phys. Rev. Lett.* **120** 016401
[54] Xiao D, Chang M C and Niu Q 2010 *Rev. Mod. Phys.* **82** 1959
[55] Nielsen H and Ninomiya M 1981 *Phys. Lett. B* **105** 2
[56] Zhang D, Shi M, Zhu T, Xing D, Zhang H and Wang J 2019 *Phys. Rev. Lett.* **122** 206401
[57] Wang L L, Jo N H, Kuthanazhi B, Wu Y, McQueeney R J, Kaminski A and Canfield P C 2019 *Phys. Rev. B* **99** 245147
[58] Soh J R, de Juan F, Vergniory M G, Schröter N B M, Rahn M C, Yan D Y, Jiang J, Bristow M, Reiss P, Blandy J N, Guo Y F, Shi Y G, Kim T K, McCollam A, Simon S H, Chen Y, Coldea A I and Boothroyd A T 2019 *Phys. Rev. B* **100** 201102
[59] Wu P, Liu G, Hu X and Xu H 2023 *Phys. Rev. B* **108** 054305
[60] Wang X, Zhou F, Zhang Z, Wu W, Yu Z M and Yang S A 2022 *Phys. Rev. B* **106** 195129
[61] Kresse G and Hafner J 1993 *Phys. Rev. B* **47** 558
[62] Kresse G and Furthmüller J 1996 *Comput. Mater. Sci.* **6** 15
[63] Hohenberg P and Kohn W 1964 *Phys. Rev.* **136** B864
[64] Kohn W and Sham L J 1965 *Phys. Rev.* **140** A1133
[65] Blöchl P E 1994 *Phys. Rev. B* **50** 17953
[66] Perdew J P, Burke K and Ernzerhof M 1996 *Phys. Rev. Lett.* **77** 17953
[67] Chaput L, Togo A, Tanaka I and Hug G 2011 *Phys. Rev. B* **84** 094302
[68] Baroni S, Gironcoli S, Corso A D and Giannozzi P 2001 *Rev. Mod. Phys.* **73** 515
[69] Lopez Sancho M P, Lopez Sancho J M, Sancho J M L and Rubio J 1985 *J. Phys. F: Metal Phys.* **15** 851
[70] Seifert K J, Nowotny H and Hauser E 1971 *Monatshefte für Chemie* **102** 1006
[71] Liu Q B, Qian Y T, Fu H H and Wang Z J 2020 *NPJ Comp. Mater.* **6** 95
[72] Wan X G, Turner M, Vishwanath A and Savrasov S Y 2011 *Phys. Rev. B* **83** 205101
[73] Xu R Q and Chiang T C 2005 *Z. Kristallogr.* **220** 1009
[74] Eichler A, Bohnen K P, Reichardt W and Hafner J 1998 *Phys. Rev. B* **57** 324
[75] Ibach H 1987 *J. Vac. Sci. Technol. A* **5** 419
[76] Lourenço-Martins H and Kociak M 2017 *Phys. Rev. X* **7** 041059
[77] Benedek G and Toennies J P 1994 *Surf. Sci.* **299** 587